Journal of Dentistry 165 (2026) 106269

Contents lists available at ScienceDirect

Journal of Dentistry

journal homepage: www.elsevier.com/locate/jdent

Trueness of extraoral photogrammetry, intraoral photogrammetry and direct intraoral scanning in the full-arch digital implant impression: a comparative *in vitro* study

Francesco Guido Mangano [a,*], Henriette Lerner [b], Gabriele Valle [c], Francesco Biaggini [c], Carlo Mangano [d], Andrey Dybov [a]

[a] Department of Pediatric, Preventive Dentistry and Orthodontics, I. M. Sechenov First State Medical University, Moscow, Russia
[b] Academic Teaching and Research Institution of Johann Wolfgang Goethe University, Frankfurt, Germany
[c] IPD Dental Group, Arcola, La Spezia, Italy
[d] Department of Dental Sciences, San Raffaele University, Milan Italy

ARTICLE INFO

Keywords:
Coordinate measuring machine
Extraoral photogrammetry
Intraoral photogrammetry
Intraoral scanners
Full-arch implant impressions
Trueness

ABSTRACT

Objective: To compare the trueness of extraoral photogrammetry (EPG), intraoral photogrammetry (IPG), and four intraoral scanners (IOSs) in capturing a completely edentulous model with six implant analogs.
Methods: A type IV plaster master model containing six implant analogs was digitized using a coordinate measuring machine (CMM) to obtain the reference dataset. The model was then scanned with two photogrammetric systems—an extraoral device (3Dots®) and an IOS equipped with IPG (Aoralscan Elite IPG®)—as well as four IOSs (TRIOS 6®, CS 3800®, iTero Lumina™, i900®). Ten scans per IOS were performed under standardized conditions. All datasets were processed in CAD software to replace scanbodies (SBs) with their corresponding library geometries and analyzed in reverse-engineering software to measure inter-implant distances. Absolute deviations from CMM data were used to assess trueness. Statistical analysis included descriptive statistics and repeated measures ANOVA with Bonferroni correction ($\alpha = 0.05$).
Results: EPG demonstrated the highest trueness (mean deviation 5 μm), followed by IPG (29 μm) and iTero Lumina™ (34 μm). The i900® (54 μm), TRIOS 6® (84 μm), and CS 3800® (223 μm) exhibited progressively greater deviations. No significant differences were observed among EPG, IPG, and iTero Lumina™, which all outperformed TRIOS 6® ($p \leq 0.020$) and CS 3800® ($p < .001$). Medit i900® and TRIOS 6® were also significantly more accurate than CS 3800® ($p < .001$). Segment-level analysis revealed higher deviations for longer inter-implant spans.
Conclusions: Within the limits of this study, EPG achieved the highest accuracy and remains the reference method for full-arch implant digitization. IPG and iTero Lumina™ reached comparably high trueness, followed by Medit i900® and TRIOS 6®.
Clinical Relevance: Next-generation IOSs, particularly iTero Lumina™, may approach the trueness of photogrammetric systems, although photogrammetry—especially EPG—remains the most accurate option for digital full-arch implant acquisition.

1. Introduction

Intraoral scanners (IOSs) have revolutionized implant prosthodontics by enabling the acquisition of accurate optical impressions [1–3]. These digital datasets can be processed through computer-aided design (CAD) and subsequently manufactured via

Abbreviations: EPG, extraoral photogrammetry; IPG, intraoral photogrammetry; IOS, intraoral scanner; CMM, coordinate measuring machine; CAD, computer assisted design; SB, scanbody; CAM, computer assisted manufacturing; FA, full arch; 3D, three dimensional; MUA, multi-unit abutment; STL, standard tessellation language.

* Corresponding author at: Department of Pediatric, Preventive Dentistry and Orthodontics, I. M. Sechenov First State Medical University, Moscow, Russia.
E-mail addresses: francescoguidomangano@gmail.com (F.G. Mangano), h-lerner@web.de (H. Lerner), gvalle@ipd2004.com (G. Valle), francesco.biaggini@me.com (F. Biaggini), camangan@gmail.com (C. Mangano), dybov_a_m@staff.sechenov.ru (A. Dybov).

https://doi.org/10.1016/j.jdent.2025.106269
Received 30 October 2025; Received in revised form 18 November 2025; Accepted 22 November 2025
Available online 27 November 2025

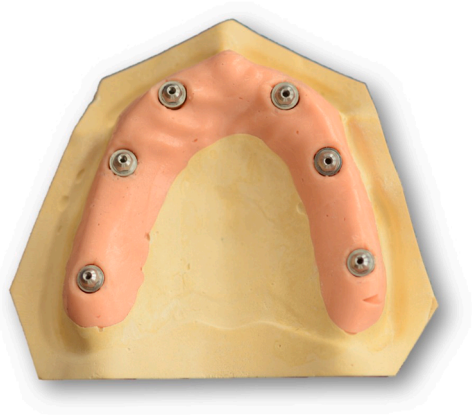

Fig. 1. A type IV dental stone master model was fabricated featuring six implant analogs with MUAs (IPD/AB-AR-00®, IPD Dental, Matarò, Barcelona, Spain), positioned in an approximately parallel alignment at sites #16, #14, #12, #22, #24, and #26.

computer-aided manufacturing (CAM), facilitating the production of implant-supported restorations with clinically acceptable precision [3–6]. Such workflows apply to a wide range of indications, from single crowns to multi-unit fixed partial dentures, and can employ various restorative materials [4–6].

However, the clinical use of IOSs in fully edentulous patients requiring implant-supported full-arch (FA) rehabilitations remains challenging and is still the subject of debate [7–9]. Current evidence is inconclusive regarding whether IOSs can achieve the accuracy required for these complex rehabilitations [8,10]. Several systematic reviews have suggested that IOSs may be intrinsically unsuitable for this indication due to the cumulative effect of stitching errors and inherent accuracy limitations [9–11]. Clinical reports further support these concerns, particularly in mandibular cases, where the absence of palatal landmarks and interference from the tongue complicate intraoral scanning [12].

Despite these limitations, some clinical studies have reported successful outcomes using IOSs for FA implant-supported rehabilitations [13,14]. Imburgia et al. [14] demonstrated the feasibility of fabricating monolithic zirconia FA prostheses through a fully digital workflow based on direct implant scanning. Their 'Continuous Scan Strategy,' which involved splinting implant scan bodies (SBs) with thermoplastic resin, enabled the delivery of 35 monolithic zirconia FA prostheses—extraorally cemented onto modified, short titanium bases—with clinically acceptable accuracy [14]. The authors emphasized, however, that predictable outcomes depend on strict control of multiple variables influencing the transfer of three-dimensional (3D) implant positions from the patient to the CAD environment [14]. These factors include the intrinsic accuracy of the IOS [15,16], the operator's scanning strategy and experience [17], environmental conditions such as lighting and temperature [18,19], patient-related factors such as implant number, depth, and distribution [20], the type of SBs used [21,22], the geometric congruence between SB meshes and implant library files [23,24], and the milling precision of zirconia–titanium interfaces. Achieving optimal accuracy across these stages is feasible but demands substantial clinical and technical expertise [14–24].

Following this work, the concept of splinting SBs has gained growing attention [25,26]. Building on this principle, several innovations have been developed, including novel connection systems [26], prefabricated splinting frameworks [27], and modified SB designs—"scan gauges"—that extend horizontally rather than vertically [28]. These designs, connected to multi-unit abutments (MUAs), minimize vertical wand movement, reduce inter-SB gaps, and guide the scanning process, thereby improving accuracy [28]. Such systems have demonstrated promising clinical results, enabling accurate fabrication of monolithic FA prostheses [26–28], although they introduce additional procedural steps and increased costs.

An effective alternative is extraoral photogrammetry (EPG) [29–34], a 3D acquisition technique employing stereophotogrammetric systems to capture the spatial position of dental implants through simultaneous registration of high-resolution images of dedicated markers [29,30]. The subsequent algorithmic processing determines the 3D coordinates and angular relationships of implants relative to a reference system, producing a digital file that can be directly integrated into CAD/CAM workflows for FA restoration design and fabrication [29,32]. Although recent clinical investigations have confirmed the accuracy of EPG [33,34], its widespread adoption remains limited due to higher costs and procedural complexity. In fact, EPG captures only the position of the implants, but not the soft tissues; for capturing the soft tissues, IOS

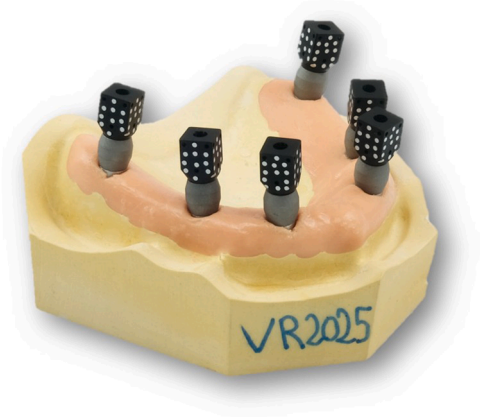

Fig. 3. The plaster model was prepared for acquisition with the EPG system (3Dots®, OpenTech, Brescia, Italy), which uses stereophotogrammetry with dual high-resolution cameras to capture implant coordinates with micron accuracy; dedicated metallic markers were secured to each analog.

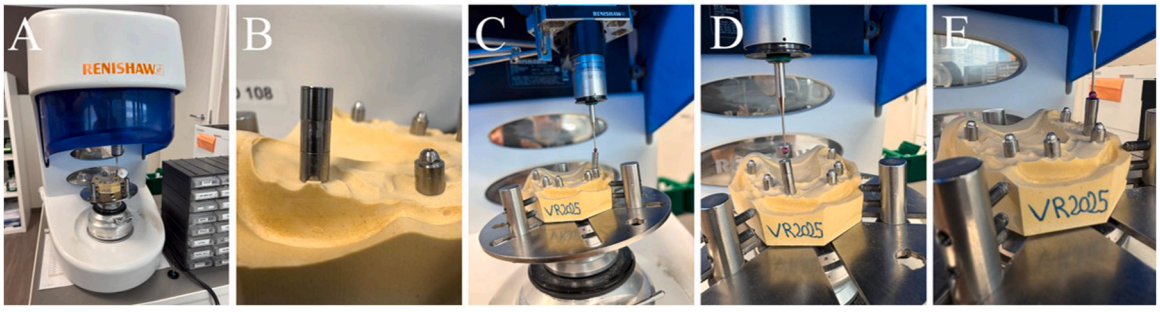

Fig. 2. The master model was then digitized using a CMM (DS 10®, Renishaw, Wotton-under-Edge, Gloucestershire, UK) equipped with an SM25–1 scanning module, an SP25M probe, and a 3 mm ruby stylus tip (M3), to generate the reference virtual model.

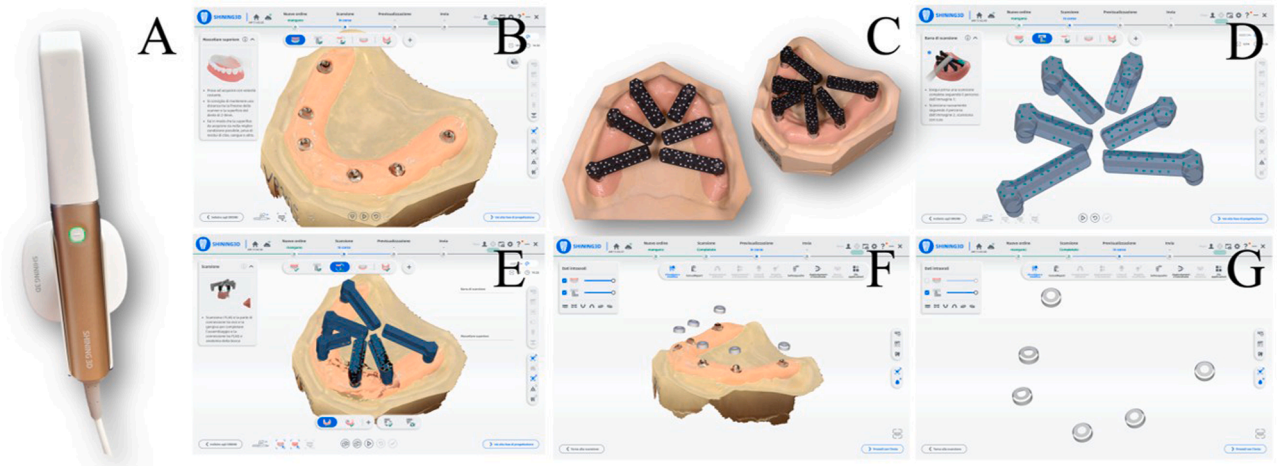

Fig. 4. IPG Scanning protocol: the model was first scanned with MUAs only, followed by a second scan with encoded scanbodies (Scanflags®, Shining 3D Dental, Hangzhou, China) using the photogrammetry mode. The software aligned and merged the datasets, incorporating the implant library geometries (IPD Dental, Matarò, Barcelona, Spain) to generate the final STL model with precisely positioned scanbody coordinates.

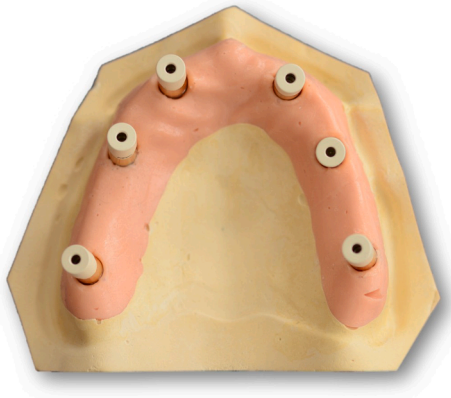

Fig. 5. Replacement of Scanflags® with conventional cylindrical MUA scanbodies (IPD/AB-SR-01®, IPD Dental, Matarò, Barcelona, Spain).

scanning is still needed, and this data must then be combined in a single 3D model, using specific algorithms [33,34].

Intraoral photogrammetry (IPG) represents an emerging technology that integrates videoophotogrammetric principles directly into the IOS, as exemplified by the Aoralscan Elite IPG® (Shining 3D) [35,36]. This system enables direct capture of the 3D spatial position and orientation of implant markers intraorally, eliminating the need for external cameras. Compared with EPG, IPG offers a more streamlined workflow, fewer procedural steps, and greater clinical efficiency, while maintaining accuracy levels that recent *in vitro* studies have found to be clinically acceptable [35,36]. However, clinical evidence supporting these results remains scarce [34].

More recently, IOS manufacturers have introduced new scanners claiming improved accuracy for direct implant scanning without the use of special SBs, connection frameworks, or photogrammetry [37–39]. TRIOS 6® from 3Shape features advanced multi-modal imaging, hyperspectral technology, and AI-powered diagnostics to deliver high-resolution scans. Its technological capabilities include the simultaneous use of white light, fluorescence, and near-infrared light to

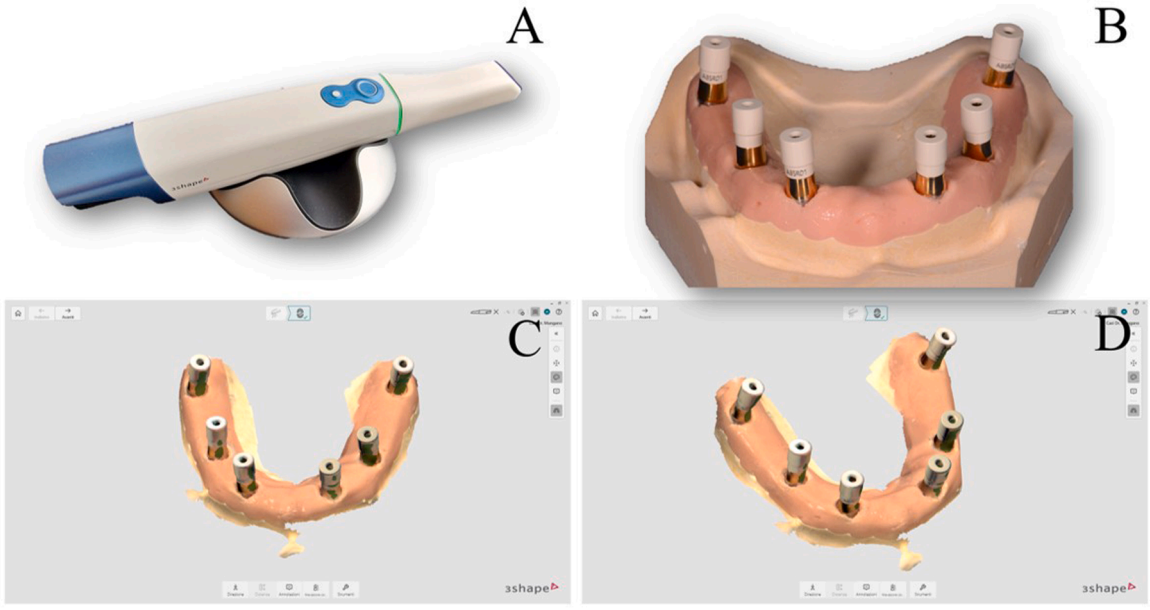

Fig. 6. Model acquisition using TRIOS 6® (3Shape, Copenhagen, Denmark).

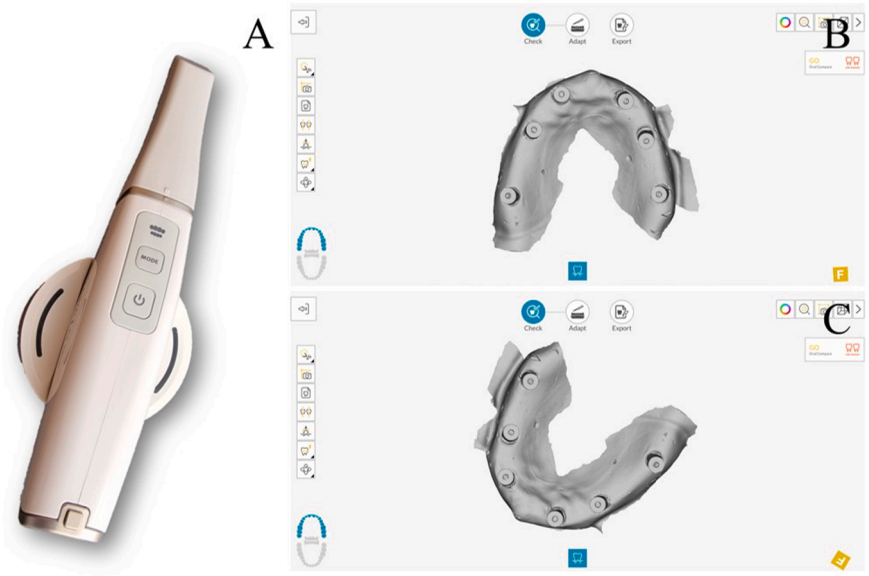

Fig. 7. Model acquisition using CS 3800® (Carestream Dental, Atlanta, GA, USA).

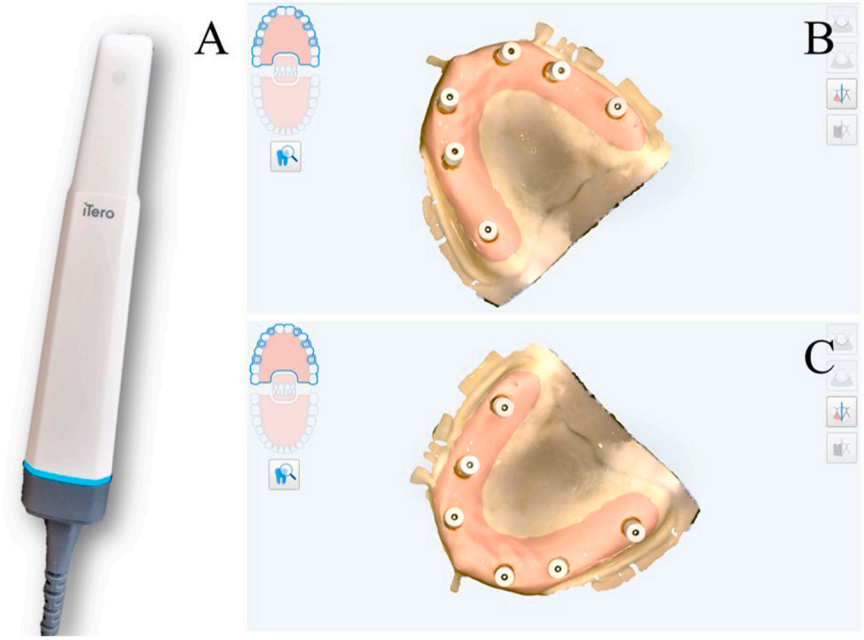

Fig. 8. Model acquisition using iTero Lumina™ (Align Technology Inc, San José, CA, USA).

generate highly detailed images [37]. The i900® is Medit's newest IOS, equipped with a third-generation optical engine designed to improve scanning speed, depth of field (up to 30 mm), and color accuracy [37, 38]. Finally, the iTero Lumina™ scanner, released by Align Technology, incorporates proprietary Multi-Direct Capture Technology, which collects data from multiple optical paths at the same time, thereby increasing the amount of surface information captured per unit time [39]. This innovation has the potential to enhance accuracy, depth of field, and scanning efficiency in FA applications [39].

The aim of this *in vitro* study was to compare the trueness of different scanning systems—namely EPG, IPG, and direct scanning with various IOSs—in a completely edentulous model with six implant analogs.

2. Materials and methods

2.1. Master model and precision probing

A type IV plaster master model was fabricated incorporating six MUAs implant analogs (IPD/AB-AR-00®, IPD Dental, Matarò, Barcelona, Spain), placed in an approximately parallel configuration at sites #16, #14, #12, #22, #24, and #26 (Fig. 1).

This model was subsequently digitized to obtain a reference virtual model using a coordinate measuring machine (CMM) (DS 10®, Renishaw, Wotton Under Edge, Gloucestershire, UK), equipped with an SM25–1 module, an SP25M probe, and a ruby stylus tip (M3, 3 mm diameter) (Fig. 2). The plaster model was fixed onto the specimen holder of the DS10. Metallic cylindrical SBs were screwed onto each analog, with manual tightening and mechanical stability carefully verified.

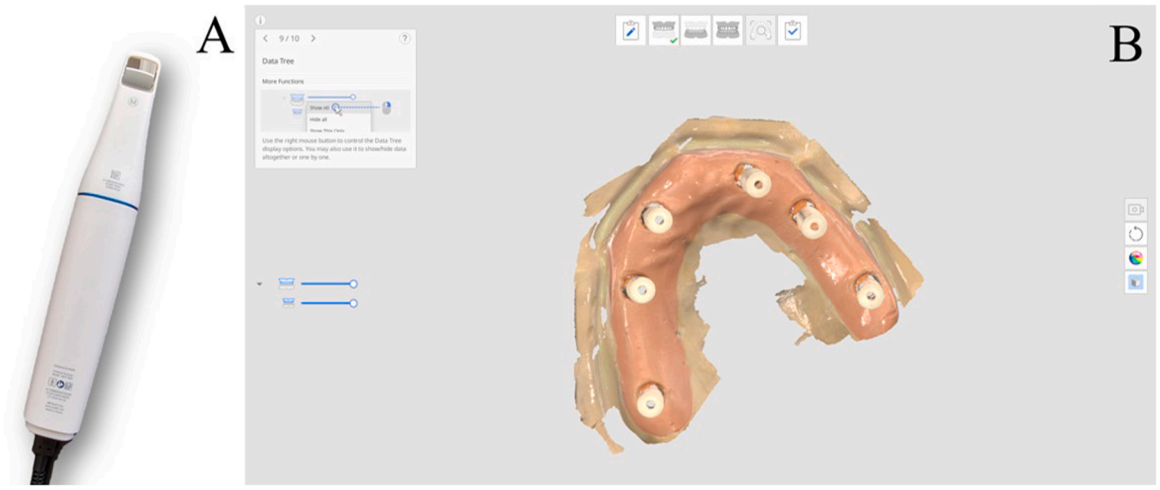

Fig. 9. Model acquisition using i-900® (Medit, Seoul, South Korea).

Given the fragility of plaster, particular attention was paid to avoid chipping or microfractures during tightening. A reference system was then defined. The operator manually positioned the probe near three reference points on the supporting plane of the model. These points were measured to establish the coordinate system (origin and XYZ axes). The probing sequence was subsequently programmed. With the reference system activated, the operator instructed the software regarding the geometry of the metallic SBs:

- External cylinder: 6 equidistant points along the circumference for each implant
- Upper plane: 1 central point, to define height and vertical axis

The sequence was saved as a FA measurement routine. Automatic probing was then carried out. The DS10® performed the measurement of all six implants automatically:

- Progressive approach
- Contact of the ruby sphere with the selected point
- Recording of the coordinate
- Movement to the next point

The complete cycle required approximately 15 min, including repositioning movements. Data validation and export were then performed. To assess stability, two implants (#16 and #26) were probed twice. The differences between the two acquisitions fell within laboratory tolerances. The probing data were exported in standard tessellation language (STL) format. Upon importing the file into CAD (Elefsina 3.2®, exocad, Darmstadt, Germany), implant axes were recognized using the dedicated library.

2.2. Extraoral photogrammetry (EPG)

The plaster model was then ready for the EPG (3Dots®, OpenTech, Brescia, Italy) acquisition to begin. 3Dots® is an EPG system, based on stereophotogrammetry, where two high-resolution industrial cameras and the geometric triangulation performed by the software return with micron precision the exact 3D coordinates of the implants. The dedicated EPG metallic markers were screwed onto each analog, verifying manual tightening and mechanical stability (Fig. 3). It was not necessary to define any reference system. 3Dots® was held at about 35 cm from the plaster model and the photogrammetric acquisition was started by moving the scanner at a constant distance while keeping the model in the center of the rotation circle. The movement covered an excursion of about 30°, centered on the frontal position (approximately 15° to the right and 15° to the left) (Videos 1,2). The total scanning time was about 15 s. Data was then processed by the Optor L Ultra® (OpenTech, Brescia, Italy) software. The Optor L Ultra® software included with 3Dots® enables the automatic determination of implant positions, based on the data acquired through 3Dots® and from an implant library specified by the operator. The implant geometries positioned by the Optor L Ultra® software were exported in standard STL format, and saved in a dedicated folder. The sequence was repeated five times.

2.3. Intraoral photogrammetry (IPG)

At this stage, the metallic markers were removed, and the plaster model was positioned inside the head of a mannequin to simulate intraoral lighting conditions. For IPG, the device employed was the Aoralscan Elite IPG® (Shining 3D Dental, Hangzhou, China). The software version used was IntraoralScan 3.5.6.9. In total, ten scans were performed by an experienced operator (F.G.M) with >15 years of expertise in direct intraoral scanning (Fig. 4). The scanning protocol was as follows: initially, the operator scanned the model with the MUAs in place, without any SB. Subsequently, encoded SBs specifically designed for IPG (Scanflags®, Shining 3D Dental, Hangzhou, China) were screwed onto the MUAs, in order to fill the gaps and reduce the inter-implant distances, and the model was rescanned using the photogrammetry modality. The scan with Scanflags® was performed from above, at a preconfigured distance, moving from right to left. The software then executed the matching process, aligning the photogrammetric data with the model containing the MUAs, and merging the datasets. The operator subsequently selected the requested implant CAD library geometries (IPD Dental, Matarò, Barcelona, Spain), and the software optimized the dataset by generating both the STL surface of the model and the corresponding SB geometries, precisely positioned in the XYZ coordinates. In total, the operator captured 10 scans with Aoralscan Elite IPG®, therefore ten STL files with the CAD libraries of the SBs were saved in a dedicated folder, each labeled according to the technology used (IPG) and sequentially numbered from 1 to 10.

2.4. Direct intraoral scanning

After completing 10 acquisitions with IPG technology, the Scanflags® were removed and replaced with conventional cylindrical MUA SBs (IPD/AB-SR-01®, IPD Dental, Matarò, Barcelona, Spain) (Fig. 5). Using these, the same experienced operator performed 10 direct digital scans per group with four different intraoral scanners (IOSs: TRIOS 6®, 3Shape, Copenhagen, Denmark; CS 3800®, Carestream Dental, Atlanta, GA, USA; iTero Lumina™, Align Technology Inc, San José, CA, USA; and

Table 1
Descriptive analysis (absolute error in mm).

		Min	Max	Mean	SD	Median	P25	P75
TRIOS 6®	#12-#22	.0130	.0932	.0415	.0250	.0413	.0218	.0522
	#12-#26	.0051	.1919	.1143	.0590	.1051	.0775	.1752
	#14-#12	.0031	.0621	.0284	.0193	.0269	.0108	.0423
	#16-#12	.0019	.0700	.0304	.0254	.0267	.0105	.0490
	#16-#14	.0004	.5293	.0702	.1625	.0164	.0045	.0357
	#16-#22	.0213	.1229	.0814	.0354	.0837	.0540	.1175
	#16-#26	.1189	.5074	.3378	.1351	.3720	.2665	.4450
	#22-#24	.0312	.0755	.0500	.0153	.0482	.0349	.0636
	#22-#26	.0257	.1156	.0631	.0282	.0555	.0464	.0744
	#24-#26	.0011	.0380	.0213	.0126	.0240	.0136	.0315
CS 3800®	#12-#22	.0076	.1389	.0615	.0398	.0544	.0352	.0884
	#12-#26	.0542	.3155	.1491	.0882	.1254	.0702	.1943
	#14-#12	.0137	.1312	.0666	.0307	.0636	.0516	.0823
	#16-#12	.2093	.5395	.3953	.0993	.4149	.3299	.4711
	#16-#14	.1660	.4754	.3430	.1001	.3649	.2498	.4164
	#16-#22	.2421	.7837	.4450	.1469	.4126	.3773	.4618
	#16-#26	.0614	.7713	.2709	.1901	.2504	.1849	.2710
	#22-#24	.0441	.2247	.0979	.0580	.0766	.0613	.1173
	#22-#26	.0213	.3684	.2372	.1022	.2259	.1868	.3105
	#24-#26	.0884	.2910	.1672	.0663	.1558	.1258	.1996
EPG	#12-#22	.0000	.0000	.0000	.	.0000	.0000	.0000
	#12-#26	.0008	.0008	.0008	.	.0008	.0008	.0008
	#14-#12	.0059	.0059	.0059	.	.0059	.0059	.0059
	#16-#12	.0131	.0131	.0131	.	.0131	.0131	.0131
	#16-#14	.0054	.0054	.0054	.	.0054	.0054	.0054
	#16-#22	.0004	.0004	.0004	.	.0004	.0004	.0004
	#16-#26	.0006	.0006	.0006	.	.0006	.0006	.0006
	#22-#24	.0015	.0015	.0015	.	.0015	.0015	.0015
	#22-#26	.0106	.0106	.0106	.	.0106	.0106	.0106
	#24-#26	.0121	.0121	.0121	.	.0121	.0121	.0121
iTero Lumina™	#12-#22	.0332	.0875	.0559	.0153	.0543	.0473	.0639
	#12-#26	.0046	.1048	.0406	.0334	.0370	.0071	.0626
	#14-#12	.0065	.0300	.0161	.0076	.0138	.0114	.0228
	#16-#12	.0038	.0567	.0210	.0156	.0147	.0111	.0269
	#16-#14	.0035	.0511	.0209	.0170	.0136	.0074	.0355
	#16-#22	.0118	.0627	.0328	.0170	.0281	.0192	.0451
	#16-#26	.0084	.1331	.0754	.0458	.0846	.0361	.1116
	#22-#24	.0005	.0307	.0136	.0112	.0125	.0025	.0244
	#22-#26	.0045	.0707	.0422	.0257	.0437	.0146	.0640
	#24-#26	.0004	.0378	.0214	.0126	.0239	.0150	.0278
i900®	#12-#22	.0322	.0468	.0394	.0052	.0398	.0338	.0432
	#12-#26	.0168	.0567	.0351	.0128	.0350	.0272	.0384
	#14-#12	.0018	.0166	.0057	.0050	.0035	.0024	.0074
	#16-#12	.0381	.0797	.0641	.0180	.0730	.0401	.0781
	#16-#14	.0350	.0848	.0646	.0189	.0699	.0459	.0779
	#16-#22	.0487	.0927	.0801	.0151	.0865	.0730	.0903
	#16-#26	.1099	.1500	.1292	.0125	.1300	.1188	.1375
	#22-#24	.0018	.0255	.0183	.0068	.0186	.0173	.0230
	#22-#26	.0167	.0861	.0633	.0196	.0640	.0568	.0778
	#24-#26	.0100	.0534	.0381	.0142	.0362	.0293	.0529
Aoralscan Elite IPG®	#12-#22	.0394	.0537	.0468	.0048	.0483	.0426	.0503
	#12-#26	.0226	.0342	.0285	.0042	.0289	.0241	.0326
	#14-#12	.0042	.0161	.0105	.0039	.0108	.0075	.0126
	#16-#12	.0159	.0290	.0219	.0041	.0217	.0188	.0250
	#16-#14	.0189	.0347	.0248	.0047	.0233	.0219	.0274
	#16-#22	.0463	.0553	.0508	.0031	.0500	.0485	.0541
	#16-#26	.0485	.0675	.0578	.0061	.0574	.0532	.0625
	#22-#24	.0220	.0263	.0238	.0013	.0237	.0229	.0244
	#22-#26	.0051	.0175	.0129	.0040	.0136	.0103	.0159
	#24-#26	.0039	.0161	.0098	.0037	.0099	.0086	.0123

i-900®, Medit, Seoul, South Korea) (Figs. 6,7,8,9). IOSs were calibrated prior to scanning using the respective manufacturer's calibration systems, when available. A randomized scanning sequence was adopted to minimize operator fatigue. The models were scanned inside the mannequin head to simulate lighting conditions comparable to those encountered clinically in the intraoral environment. In all cases, the operator followed a standardized scanning protocol: an initial pass along the occlusal surface from right to left, a return pass along the buccal side from left to right, and a final pass along the palatal side from right to left. The total duration of each scan was limited to a maximum of 35 s in order to reduce or prevent scanbody mesh distortion, which tends to increase with prolonged scanning. Additionally, all scans were acquired under standardized environmental conditions, in a room maintained at 21 °C, 45 % relative humidity, and an air pressure of 750 ± 5 mmHg. The datasets were saved in STL format. For each IOS, 10 virtual models were generated, resulting in a total of 40 STL files. These files were stored in dedicated folders, each labeled according to the IOS used and sequentially numbered from 1 to 10.

2.5. CAD procedures and outcome variables

Subsequently, all scans were processed using CAD software (Elefsina

Table 2
Error estimates for the different scanners (in mm).

Measure: Points				
Equipment	Mean	Std. Error	95 % Confidence Interval	
			Lower Bound	Upper Bound
TRIOS 6® (3 SHAPE)	.084	.007	.070	.098
CS 3800® (CARESTREAM)	.223	.007	.209	.237
EPG	.005	.022	−0.039	.049
iTero Lumina™ (ALIGN)	.034	.007	.020	.048
i900® (MEDIT)	.054	.007	.040	.068
AoralScan Elite IPG® (SHINING 3D)	.029	.007	.015	.043

3.2®, exocad, Darmstadt, Germany). A master dental technician (G.V.), with over 25 years of CAD experience, performed all laboratory procedures. The scans were cleaned using a predefined template, after which the operator replaced each SB mesh with the corresponding CAD library file (IPD/AB-AR-00®, IPD Dental, Matarò, Barcelona, Spain) thereby producing STL files in which all six SBs were represented by their original library-derived geometries in their respective spatial positions. This procedure yielded 40 new STL files (10 per group, for the direct intraoral scanning groups). Screenshots were saved representing each group of scanners. This procedure was performed inside the CAD software, also for the data released by EPG and IPG, even if these systems already provided the STL files with the CAD libraries in position as functional output.

These datasets were subsequently imported into reverse engineering software (Inspect 2025®, Zeiss, Oberkochen, Germany) to compute inter-SB distances (segment lengths, i.e. the specific length of each of #12–#22, #12–#26, #14–#12, #16–#12, #16–#14, #16–#22, #16–#26, #22–#24, #22–#26, #24–#26). The resulting measurements were tabulated in a dedicated worksheet (Excel®, Microsoft, Redmond, USA) and compared against the reference touch-probe CMM data to determine the absolute error of each segment, in mm. Ultimately, the absolute error present in linear segments and cross-sections (#12–#22, #12–#26, #14–#12, #16–#12, #16–#14, #16–#22, #16–#26, #22–#24, #22–#26, #24–#26) represented the main outcome of the study, which aimed to highlight and compare the intrinsic trueness of the different technologies (EPG, IPG and direct implant scanning, with different IOSs), both at the overall level and for each of the specificly measured linear and cross segments.

2.6. Statistical analysis

A descriptive analysis was first performed for each equipment, including the calculation of mean, standard deviation, median, minimum and maximum values, as well as the 25th and 75th percentiles. A repeated measures ANOVA was then conducted to compare the performance of the different technologies. The within-subject factor was the points (i.e., (#12–#22, #12–#26, #14–#12, #16–#12, #16–#14, #16–#22, #16–#26, #22–#24, #22–#26, #24–#26), while the between-subject factor was the equipment (TRIOS 6®, CS 3800®, EPG, iTero Lumina™, i900®, Aoralscan Elite IPG®). Mauchly's test was used to verify the assumption of sphericity and when this assumption was violated, the Greenhouse–Geisser correction was applied. A post-hoc analysis with Bonferroni correction was performed to explore pairwise differences. A p-value < 0.05 was considered statistically significant. All analyses were performed using IBM SPSS Statistics, version 30.

Table 3
Pairwise Comparisons between the different scanners.

Measure: Points						
(I) Technology	(J) Technology	Mean Difference (I-J)	Std. Error	Sig. [b]	95 % Confidence Interval for Difference [b]	
					Lower Bound	Upper Bound
TRIOS 6®	CS 3800®	−0.140*	.010	<0.001	−0.170	−0.109
	EPG	.079*	.023	.020	.007	.150
	iTero Lumina™	.050*	.010	<0.001	.019	.080
	i900®	.030	.010	.056	.000	.060
	AoralScan Elite IPG®	.055*	.010	<0.001	.025	.086
CS 3800®	TRIOS 6®	.140*	.010	<0.001	.109	.170
	EPG	.218*	.023	<0.001	.147	.290
	iTero Lumina™	.189*	.010	<0.001	.159	.220
	i900®	.170*	.010	<0.001	.139	.200
	AoralScan Elite IPG®	.195*	.010	<0.001	.164	.225
EPG	TRIOS 6®	−0.079*	.023	.020	−0.150	−0.007
	CS 3800®	−0.218*	.023	<0.001	−0.290	−0.147
	iTero Lumina™	−0.029	.023	1.000	−0.100	.042
	i900®	−0.049	.023	.598	−0.120	.023
	AoralScan Elite IPG®	−0.024	.023	1.000	−0.095	.048
iTero Lumina™	TRIOS 6®	−0.050*	.010	<0.001	−0.080	−0.019
	CS 3800®	−0.189*	.010	<0.001	−0.220	−0.159
	EPG	.029	.023	1.000	−0.042	.100
	i900®	−0.020	.010	.747	−0.050	.011
	AoralScan Elite IPG®	.005	.010	1.000	−0.025	.036
i900®	TRIOS 6®	−0.030	.010	.056	−0.060	.000
	CS 3800®	−0.170*	.010	<0.001	−0.200	−0.139
	EPG	.049	.023	.598	−0.023	.120
	iTero Lumina™	.020	.010	.747	−0.011	.050
	AoralScan Elite IPG®	.025	.010	.215	−0.005	.055
AoralScan Elite IPG®	TRIOS 6®	−0.055*	.010	<0.001	−0.086	−0.025
	CS 3800®	−0.195*	.010	<0.001	−0.225	−0.164
	EPG	.024	.023	1.000	−0.048	.095
	iTero Lumina™	−0.005	.010	1.000	−0.036	.025
	i900®	−0.025	.010	.215	−0.055	.005

Based on estimated marginal means.
* The mean difference is significant at the 0.05 level.
[b] Adjustment for multiple comparisons: Bonferroni.

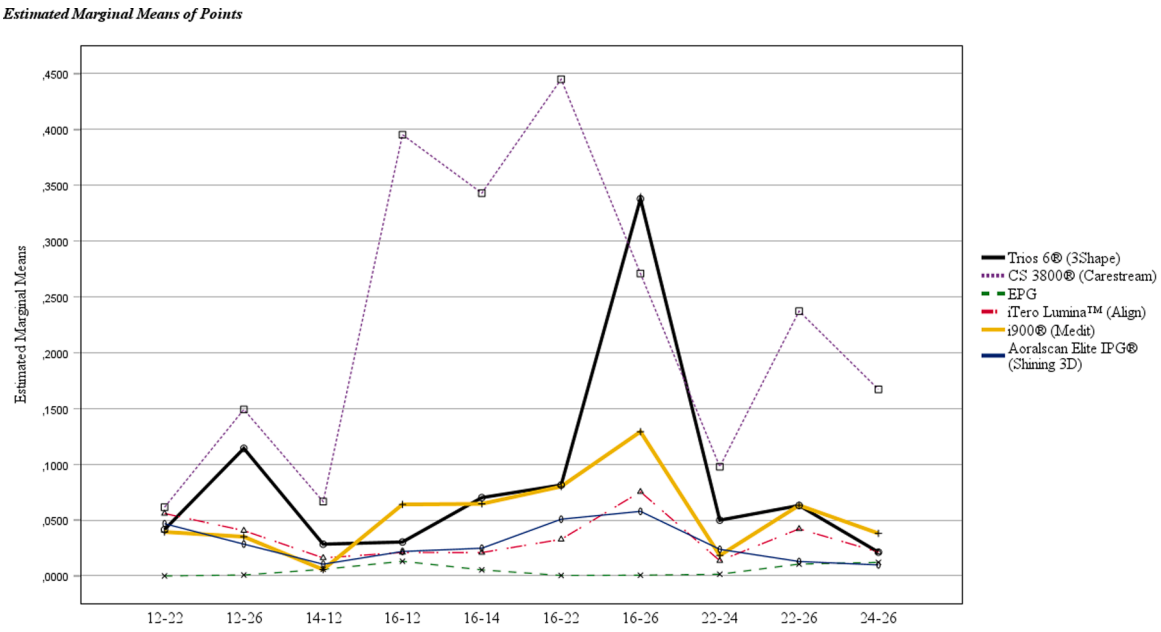

Fig. 10. Repeated measures ANOVA showed no significant differences among EPG, Aoralscan Elite IPG®, and iTero Lumina™. EPG exhibited significantly higher accuracy than TRIOS 6® ($p = .020$) and CS 3800® ($p < .001$), while Aoralscan Elite IPG® and iTero Lumina™ also outperformed TRIOS 6® and CS 3800® ($p < .001$). Medit i900® and TRIOS 6® were more accurate than CS 3800® only ($p < .001$), which showed the lowest accuracy overall ($p < .001$).

Table 4
Error estimates of the different segments (in mm).

Estimates				
Measure: Points				
Factor1	Mean	Std. Error	95 % Confidence Interval	
			Lower Bound	Upper Bound
#12-#22	.041	.005	.032	.050
#12-#26	.061	.010	.041	.082
#14-#12	.022	.003	.015	.029
#16-#12	.091	.010	.072	.110
#16-#14	.088	.018	.053	.124
#16-#22	.115	.014	.087	.143
#16-#26	.145	.022	.102	.189
#22-#24	.034	.006	.023	.045
#22-#26	.072	.010	.051	.092
#24-#26	.045	.006	.032	.058

3. Results

Mauchly's test of sphericity was statistically significant ($W = 0.000$, Chi-square (44) = 443.571, p-value <0.001), therefore the Greenhouse-Geisser correction was used ($\varepsilon = 0.321$).

The results of the descriptive analysis are reported in Table 1. At the mean error level, when considering the entire set of segments, the highest accuracy was achieved by EPG (mean error: 5 μm). This was followed by IPG (mean error: 29 μm), and, among the IOSs, by iTero Lumina™ (34 μm). Subsequent values were recorded for the i900® (mean error: 54 μm), the TRIOS 6® (84 μm), and, lastly, the CS 3800® (223 μm) (Table 2). A repeated measures ANOVA was performed to compare the performance of the different scanners (Table 3, Fig. 10). The analysis revealed that there were no statistically significant differences among EPG, Aoralscan Elite IPG® and iTero Lumina™. Specifically, EPG demonstrated significantly higher accuracy than TRIOS 6® ($p = .020$) and CS 3800® ($p < .001$), and was therefore similar to Aoralscan Elite IPG® and iTero Lumina™, which were also significantly more accurate than TRIOS 6® ($p < .001$) and CS 3800® ($p < .001$). Medit i900® and TRIOS 6® were significantly more accurate than CS 3800® only ($p < .001$). Finally, CS 3800® was found to be significantly less accurate than all other scanners ($p < .001$).

Table 4 presents the estimates for the different segments, and Table 5 reports the comparative analysis among the different segments. Considering the overall means across points, segment #12–#22 showed significantly higher values than #14–#12, and significantly lower values than #16–#12, #16–#22, and #16–#26; segment #12–#26 had significantly lower values compared with #22–#24; segment #14–#12 was significantly lower than #12–#22, #16–#12, #16–#14, #16–#22, #16–#26, and #22–#26; segment #16–#12 was significantly higher than #12–#22, #14–#12, #22–#24, and #24–#26; segment #16–#22 was significantly higher than #12–#22, #14–#12, #22–#24, and #24–#26; segment #16–#26 was significantly higher than #12–#22, #12–#26, #14–#12, #22–#24, and #24–#26; and finally, segment #22–#26 was significantly higher than #14–#12, #22–#24, and #24–#26. These results were based on estimated marginal means, with Bonferroni adjustment for multiple comparisons.

Finally, the analysis of pairwise comparisons between the technologies (Table 6) reported that: for segment #12–#22, there were no significant differences between the technologies; for segment #12–#26, TRIOS 6® and CS 3800® showed higher errors than iTero Lumina™, i900® and AoralScan Elite IPG®; for segments #14–#12, #16–#12, #16–#14, #16–#22, #22–#24, #22–#26, and #24–#26, CS 3800® had significantly higher errors than all other scanners; for segment #16–#26, TRIOS 6® showed significantly higher values than iTero Lumina™, i900® and AoralScan Elite IPG®, while CS 3800® had significantly higher delta values than iTero Lumina™ and AoralScan Elite IPG®.

4. Discussion

Intraoral scanning for the fabrication of FA implant-supported restorations remains a topic of considerable debate [7–9]. Several recent systematic reviews have highlighted the ongoing challenges and limitations associated with achieving accurate FA implant impressions using direct intraoral scanning [9–11]. These difficulties particularly persist when SBs are not splinted, when corrective frameworks for scan error compensation are not employed, or when specialized SBs—such as scan gauges—are not utilized [26–28].

For this reason, EPG has emerged as a promising alternative to direct

Table 5
Pairwise comparison between the different segments.

Measure: Points						
(I) Factor1	(J) Factor1	Mean Difference (I-J)	Std. Error	Sig. [b]	95 % Confidence Interval for Difference [b]	
					Lower Bound	Upper Bound
#12-#22	#12-#26	−0.021	.012	1.000	−0.061	.020
	#14-#12	.019*	.004	<0.001	.006	.032
	#16-#12	−0.050*	.011	.001	−0.087	−0.013
	#16-#14	−0.047	.017	.402	−0.108	.013
	#16-#22	−0.074*	.014	<0.001	−0.122	−0.026
	#16-#26	−0.104*	.021	<0.001	−0.179	−0.030
	#22-#24	.007	.007	1.000	−0.017	.030
	#22-#26	−0.031	.012	.513	−0.071	.010
	#24-#26	−0.004	.008	1.000	−0.032	.024
#12-#26	#12-#22	.021	.012	1.000	−0.020	.061
	#16-#12	.039	.011	.061	−0.001	.079
	#16-#14	−0.030	.014	1.000	−0.080	.021
	#16-#22	−0.027	.023	1.000	−0.107	.054
	#16-#26	−0.054	.017	.127	−0.113	.006
	#22-#24	−0.084*	.020	.006	−0.154	−0.014
	#22-#26	.027	.011	.771	−0.011	.066
	#24-#26	−0.010	.012	1.000	−0.053	.033
	#16-#12	.016	.009	1.000	−0.016	.049
#14-#12	#12-#22	−0.019*	.004	<0.001	−0.032	−0.006
	#12-#26	−0.039	.011	.061	−0.079	.001
	#16-#12	−0.069*	.010	<0.001	−0.102	−0.035
	#16-#14	−0.066*	.017	.018	−0.126	−0.006
	#16-#22	−0.093*	.014	<0.001	−0.141	−0.045
	#16-#26	−0.123*	.021	<0.001	−0.198	−0.048
	#22-#24	−0.012	.006	1.000	−0.034	.010
	#22-#26	−0.049*	.011	.002	−0.087	−0.012
	#24-#26	−0.023	.007	.117	−0.048	.002
#16-#12	#12-#22	.050*	.011	.001	.013	.087
	#12-#26	.030	.014	1.000	−0.021	.080
	#14-#12	.069*	.010	<0.001	.035	.102
	#16-#14	.003	.016	1.000	−0.054	.059
	#16-#22	−0.024	.011	1.000	−0.061	.013
	#16-#26	−0.054	.022	.774	−0.131	.022
	#22-#24	.057*	.012	.001	.015	.099
	#22-#26	.019	.016	1.000	−0.035	.074
	#24-#26	.046*	.011	.010	.006	.086
#16-#14	#12-#22	.047	.017	.402	−0.013	.108
	#12-#26	.027	.023	1.000	−0.054	.107
	#14-#12	.066*	.017	.018	.006	.126
	#16-#12	−0.003	.016	1.000	−0.059	.054
	#16-#22	−0.027	.018	1.000	−0.089	.035
	#16-#26	−0.057	.031	1.000	−0.166	.051
	#22-#24	.054	.019	.352	−0.014	.121
	#22-#26	.017	.021	1.000	−0.058	.091
	#24-#26	.043	.019	1.000	−0.024	.110
#16-#22	#12-#22	.074*	.014	<0.001	.026	.122
	#12-#26	.054	.017	.127	−0.006	.113
	#14-#12	.093*	.014	<0.001	.045	.141
	#16-#12	.024	.011	1.000	−0.013	.061
	#16-#14	.027	.018	1.000	−0.035	.089
	#16-#26	−0.030	.017	1.000	−0.090	.029
	#22-#24	.081*	.016	<0.001	.025	.136
	#22-#26	.044	.021	1.000	−0.028	.115
	#24-#26	.070*	.016	.003	.014	.126
#16-#26	#12-#22	.104*	.021	<0.001	.030	.179
	#12-#26	.084*	.020	.006	.014	.154
	#14-#12	.123*	.021	<0.001	.048	.198
	#16-#12	.054	.022	.774	−0.022	.131
	#16-#14	.057	.031	1.000	−0.051	.166
	#16-#22	.030	.017	1.000	−0.029	.090
	#22-#24	.111*	.024	.001	.029	.193
	#22-#26	.074	.028	.504	−0.023	.171
	#24-#26	.100*	.024	.006	.017	.184
#22-#24	#12-#22	−0.007	.007	1.000	−0.030	.017
	#12-#26	−0.027	.011	.771	−0.066	.011
	#14-#12	.012	.006	1.000	−0.010	.034
	#16-#12	−0.057*	.012	.001	−0.099	−0.015
	#16-#14	−0.054	.019	.352	−0.121	.014

(continued on next page)

Table 5 (*continued*)

Measure: Points						
(I) Factor1	(J) Factor1	Mean Difference (I-J)	Std. Error	Sig. [b]	95 % Confidence Interval for Difference [b]	
					Lower Bound	Upper Bound
	#16-#22	−0.081*	.016	<0.001	−0.136	−0.025
	#16-#26	−0.111*	.024	.001	−0.193	−0.029
	#22-#26	−0.037*	.007	<0.001	−0.063	−0.012
	#24-#26	−0.011	.007	1.000	−0.037	.015
#22-#26	#12-#22	.031	.012	.513	−0.010	.071
	#12-#26	.010	.012	1.000	−0.033	.053
	#14-#12	.049*	.011	.002	.012	.087
	#16-#12	−0.019	.016	1.000	−0.074	.035
	#16-#14	−0.017	.021	1.000	−0.091	.058
	#16-#22	−0.044	.021	1.000	−0.115	.028
	#16-#26	−0.074	.028	.504	−0.171	.023
	#22-#24	.037*	.007	<0.001	.012	.063
	#24-#26	.027*	.007	.028	.001	.052
#24-#26	#12-#22	.004	.008	1.000	−0.024	.032
	#12-#26	−0.016	.009	1.000	−0.049	.016
	#14-#12	.023	.007	.117	−0.002	.048
	#16-#12	−0.046*	.011	.010	−0.086	−0.006
	#16-#14	−0.043	.019	1.000	−0.110	.024
	#16-#22	−0.070*	.016	.003	−0.126	−0.014
	#16-#26	−0.100*	.024	.006	−0.184	−0.017
	#22-#24	.011	.007	1.000	−0.015	.037
	#22-#26	−0.027*	.007	.028	−0.052	−0.001

Based on estimated marginal means.

* The mean difference is significant at the 0.05 level.

[b] Adjustment for multiple comparisons: Bonferroni.

IOS for FA implant impressions, offering superior trueness and precision under various *in vitro* [29–32] and *in vivo* [30–34] conditions. Abuduwaili et al. [29] reported that EPG systems (Icam4D®, PIC Dental®) yielded significantly lower linear and angular deviations than IOS in the FA rehabilitation of edentulous mandibular models. Similarly, in a clinical crossover study, Negreiros et al. [30] demonstrated that EPG achieved greater precision than IOS in complete-arch scanning, particularly noting that mandibular scans obtained with IOS exhibited greater precision loss. Estibalez-Recasens et al. [33] assessed the precision of an EPG system (PIC Dental®) in capturing the spatial positions of implants for FA maxillary prostheses supported by six implants. Ten edentulous patients underwent five consecutive recordings each. Analysis of the resulting STL files revealed a mean linear precision of 14.71 ± 12.2 μm, with a maximum deviation of 61 μm, and an angular precision of 0.072 ± 0.064°, with a maximum deviation of 0.345° [33]. Overall, the EPG system demonstrated a level of precision sufficient for the accurate registration of implant positions in FA rehabilitations [33]. In a systematic review with meta-analysis, Noronha et al. [31] evaluated the accuracy of EPG compared with intraoral scanning for FA implant impressions in edentulous patients. The pooled data demonstrated significantly higher trueness and precision for EPG systems than for IOSs [31]. The authors concluded that EPG provides a more reliable method for recording implant positions in FA rehabilitations, especially when multiple implants are involved [31]. These results were confirmed by another systematic review, where Pozzi et al. emphasized that EPG represents the most precise digital approach for FA implant workflows, under both clinical and laboratory conditions [32]. Despite these encouraging results, EPG systems present certain practical drawbacks. They require an additional financial investment and are unable to capture peri-implant soft tissues, thereby necessitating complementary IOS scanning [29–32].

IPG represents a recent innovation in digital implantology, integrating coded SBs and simultaneous multi-view image capture to determine the exact 3D positions of implants within a patient's arch [35–39]. The Aoralscan Elite IPG® system by Shining 3D is the first commercially available IOS to incorporate IPG technology, allowing acquisition of both soft tissue optical impressions and implant positional data in a single workflow [35,39]. Previous *in vitro* investigations have shown that IPG can achieve higher accuracy (trueness and precision) in FA implant models compared to conventional IOSs [35,36]. In fact, Aoralscan Elite IPG® outperformed four conventional IOSs in capturing a fully edentulous mandible with four MUAs [35]. Additionally, a recent comparison of intraoral versus extraoral photogrammetry systems found that the intraoral approach of the Aoralscan Elite IPG® achieved accuracy values similar to those of leading extraoral devices when recording FA implant casts [39]. These findings suggest that IPG may bridge the gap between conventional IOS limitations (e.g., cumulative stitching error over long spans) and the high-accuracy acquisition required for FA implant prosthetics. In fact, IPG may offer a streamlined and highly accurate alternative to traditional extraoral photogrammetry or impression-based techniques [35,36], and its incorporation into a compact IOS may therefore represent a significant step forward in implant prosthodontic workflows [40,41].

In recent years, some IOS manufacturers have released new generation devices that claim enhanced accuracy for direct implant scanning—eliminating the need for specialized SBs, connection frameworks, or photogrammetry systems [37–39]. Notably, the iTero Lumina™ IOS incorporates proprietary Multi-Direct Capture™ technology, which replaces the traditional confocal imaging architecture and enables simultaneous multi-angle data collection from a significantly wider field of view and extended capture distance (up to 25 mm) [39]. In practical terms, the iTero Lumina™ may allow clinicians to capture larger segments of dental arches in a single uninterrupted pass, reducing the need for repositioning or stitching-related error [39]. This innovation may therefore contribute to increased trueness, improved depth of field and enhanced scanning efficiency, particularly relevant for FA applications. However, the literature on this topic is scarce, and validation through *in vitro* and clinical research is necessary to confirm these claims in implantology [39].

The aim of our present *in vitro* study was therefore to assess the improvements in accuracy achieved by the latest generation of IOSs recently introduced to the market, and to compare the results obtained through direct digital scanning with those achievable using current EPG and IPG systems. In our *in vitro* comparative study, the EPG system (3Dots®, OpenTech, Brescia, Italy) demonstrated the highest accuracy, with a mean error of 5 μm. This was followed by the IPG system (Aoralscan Elite IPG®, Shining 3D Dental, Hangzhou, China) showing a mean error of 29 μm, and among the IOSs, the iTero Lumina™ (Align Technology) achieved the best performance (34 μm). Higher mean errors were observed for the i900® from Medit (54 μm), the Trios 6® from 3Shape (84 μm), and the old CS 3800® from Carestream Dental, which showed the lowest mean accuracy (223 μm). Therefore in our investigation, EPG reinforced its status as the benchmark technique for complete-arch digital acquisition, and overall, photogrammetry—both

Table 6
Pairwise Comparisons between the technologies.

Measure: Points							
Factor1	(I) Technology	(J) Technology	Mean Difference (I-J)	Std. Error	Sig. [b]	95 % Confidence Interval for Difference [b]	
						Lower Bound	Upper Bound
#12-#22	TRIOS 6®	CS 3800®	−0.020	.010	.757	−0.051	.011
		EPG	.041	.023	1.000	−0.031	.114
		iTero Lumina™	−0.014	.010	1.000	−0.045	.017
		i900®	.002	.010	1.000	−0.029	.033
		AoralScan Elite IPG®	−0.005	.010	1.000	−0.036	.026
	CS 3800®	TRIOS 6®	.020	.010	.757	−0.011	.051
		EPG	.062	.023	.175	−0.011	.134
		iTero Lumina™	.006	.010	1.000	−0.025	.037
		i900®	.022	.010	.475	−0.009	.053
		AoralScan Elite IPG®	.015	.010	1.000	−0.016	.046
	EPG	TRIOS 6®	−0.041	.023	1.000	−0.114	.031
		CS 3800®	−0.062	.023	.175	−0.134	.011
		iTero Lumina™	−0.056	.023	.318	−0.128	.017
		i900®	−0.039	.023	1.000	−0.112	.033
		AoralScan Elite IPG®	−0.047	.023	.775	−0.119	.026
	iTero Lumina™	TRIOS 6®	.014	.010	1.000	−0.017	.045
		CS 3800®	−0.006	.010	1.000	−0.037	.025
		EPG	.056	.023	.318	−0.017	.128
		i900®	.017	.010	1.000	−0.014	.047
		AoralScan Elite IPG®	.009	.010	1.000	−0.022	.040
	i900®	TRIOS 6®	−0.002	.010	1.000	−0.033	.029
		CS 3800®	−0.022	.010	.475	−0.053	.009
		EPG	.039	.023	1.000	−0.033	.112
		iTero Lumina™	−0.017	.010	1.000	−0.047	.014
		AoralScan Elite IPG®	−0.007	.010	1.000	−0.038	.024
	AoralScan Elite IPG®	TRIOS 6®	.005	.010	1.000	−0.026	.036
		CS 3800®	−0.015	.010	1.000	−0.046	.016
		EPG	.047	.023	.775	−0.026	.119
		iTero Lumina™	−0.009	.010	1.000	−0.040	.022
		i900®	.007	.010	1.000	−0.024	.038
#12-#26	TRIOS 6®	CS 3800®	−0.035	.022	1.000	−0.104	.035
		EPG	.113	.053	.545	−0.050	.276
		iTero Lumina™	.074*	.022	.030	.004	.143
		i900®	.079*	.022	.015	.010	.149
		AoralScan Elite IPG®	.086*	.022	.006	.016	.155
	CS 3800®	TRIOS 6®	.035	.022	1.000	−0.035	.104
		EPG	.148	.053	.107	−0.015	.311
		iTero Lumina™	.109*	.022	<0.001	.039	.178
		i900®	.114*	.022	<0.001	.044	.183
		AoralScan Elite IPG®	.121*	.022	<0.001	.051	.190
	EPG	TRIOS 6®	−0.113	.053	.545	−0.276	.050
		CS 3800®	−0.148	.053	.107	−0.311	.015
		iTero Lumina™	−0.040	.053	1.000	−0.203	.123
		i900®	−0.034	.053	1.000	−0.197	.129
		AoralScan Elite IPG®	−0.028	.053	1.000	−0.191	.135
	iTero Lumina™	TRIOS 6®	−0.074*	.022	.030	−0.143	−0.004
		CS 3800®	−0.109*	.022	<0.001	−0.178	−0.039
		EPG	.040	.053	1.000	−0.123	.203
		i900®	.005	.022	1.000	−0.064	.075
		AoralScan Elite IPG®	.012	.022	1.000	−0.057	.082
	i900®	TRIOS 6®	−0.079*	.022	.015	−0.149	−0.010
		CS 3800®	−0.114*	.022	<0.001	−0.183	−0.044
		EPG	.034	.053	1.000	−0.129	.197
		iTero Lumina™	−0.005	.022	1.000	−0.075	.064
		AoralScan Elite IPG®	.007	.022	1.000	−0.063	.076
	AoralScan Elite IPG®	TRIOS 6®	−0.086*	.022	.006	−0.155	−0.016
		CS 3800®	−0.121*	.022	<0.001	−0.190	−0.051
		EPG	.028	.053	1.000	−0.135	.191
		iTero Lumina™	−0.012	.022	1.000	−0.082	.057
		i900®	−0.007	.022	1.000	−0.076	.063
#14-#12	TRIOS 6®	CS 3800®	−0.038*	.008	<0.001	−0.061	−0.015
		EPG	.023	.018	1.000	−0.032	.077
		iTero Lumina™	.012	.008	1.000	−0.011	.036
		i900®	.023	.008	.061	−0.001	.046
		AoralScan Elite IPG®	.018	.008	.318	−0.005	.041
	CS 3800®	TRIOS 6®	.038*	.008	<0.001	.015	.061
		EPG	.061*	.018	.019	.006	.115
		iTero Lumina™	.050*	.008	<0.001	.027	.074
		i900®	.061*	.008	<0.001	.038	.084
		AoralScan Elite IPG®	.056*	.008	<0.001	.033	.079
	EPG	TRIOS 6®	−0.023	.018	1.000	−0.077	.032

(continued on next page)

Table 6 (*continued*)

Measure: Points							
Factor1	(I) Technology	(J) Technology	Mean Difference (I-J)	Std. Error	Sig. [b]	95 % Confidence Interval for Difference [b]	
						Lower Bound	Upper Bound
		CS 3800®	−0.061*	.018	.019	−0.115	−0.006
		iTero Lumina™	−0.010	.018	1.000	−0.065	.044
		i900®	.000	.018	1.000	−0.054	.055
		AoralScan Elite IPG®	−0.005	.018	1.000	−0.059	.050
	iTero Lumina™	TRIOS 6®	−0.012	.008	1.000	−0.036	.011
		CS 3800®	−0.050*	.008	<0.001	−0.074	−0.027
		EPG	.010	.018	1.000	−0.044	.065
		i900®	.010	.008	1.000	−0.013	.034
		AoralScan Elite IPG®	.006	.008	1.000	−0.018	.029
	i900®	TRIOS 6®	−0.023	.008	.061	−0.046	.001
		CS 3800®	−0.061*	.008	<0.001	−0.084	−0.038
		EPG	.000	.018	1.000	−0.055	.054
		iTero Lumina™	−0.010	.008	1.000	−0.034	.013
		AoralScan Elite IPG®	−0.005	.008	1.000	−0.028	.018
	AoralScan Elite IPG®	TRIOS 6®	−0.018	.008	.318	−0.041	.005
		CS 3800®	−0.056*	.008	<0.001	−0.079	−0.033
		EPG	.005	.018	1.000	−0.050	.059
		iTero Lumina™	−0.006	.008	1.000	−0.029	.018
		i900®	.005	.008	1.000	−0.018	.028
#16-#12	TRIOS 6®	CS 3800®	−0.365*	.021	<0.001	−0.430	−0.300
		EPG	.017	.049	1.000	−0.136	.170
		iTero Lumina™	.009	.021	1.000	−0.056	.075
		i900®	−0.034	.021	1.000	−0.099	.032
		AoralScan Elite IPG®	.008	.021	1.000	−0.057	.074
	CS 3800®	TRIOS 6®	.365*	.021	<0.001	.300	.430
		EPG	.382*	.049	<0.001	.229	.535
		iTero Lumina™	.374*	.021	<0.001	.309	.440
		i900®	.331*	.021	<0.001	.266	.397
		AoralScan Elite IPG®	.373*	.021	<0.001	.308	.439
	EPG	TRIOS 6®	−0.017	.049	1.000	−0.170	.136
		CS 3800®	−0.382*	.049	<0.001	−0.535	−0.229
		iTero Lumina™	−0.008	.049	1.000	−0.161	.145
		i900®	−0.051	.049	1.000	−0.204	.102
		AoralScan Elite IPG®	−0.009	.049	1.000	−0.162	.144
	iTero Lumina™	TRIOS 6®	−0.009	.021	1.000	−0.075	.056
		CS 3800®	−0.374*	.021	<0.001	−0.440	−0.309
		EPG	.008	.049	1.000	−0.145	.161
		i900®	−0.043	.021	.702	−0.108	.022
		AoralScan Elite IPG®	−0.001	.021	1.000	−0.066	.064
	i900®	TRIOS 6®	.034	.021	1.000	−0.032	.099
		CS 3800®	−0.331*	.021	<0.001	−0.397	−0.266
		EPG	.051	.049	1.000	−0.102	.204
		iTero Lumina™	.043	.021	.702	−0.022	.108
		AoralScan Elite IPG®	.042	.021	.770	−0.023	.107
	AoralScan Elite IPG®	TRIOS 6®	−0.008	.021	1.000	−0.074	.057
		CS 3800®	−0.373*	.021	<0.001	−0.439	−0.308
		EPG	.009	.049	1.000	−0.144	.162
		iTero Lumina™	.001	.021	1.000	−0.064	.066
		i900®	−0.042	.021	.770	−0.107	.023
#16-#14	TRIOS 6®	CS 3800®	−0.273*	.039	<0.001	−0.392	−0.153
		EPG	.065	.090	1.000	−0.215	.345
		iTero Lumina™	.049	.039	1.000	−0.070	.169
		i900®	.006	.039	1.000	−0.114	.125
		AoralScan Elite IPG®	.045	.039	1.000	−0.074	.165
	CS 3800®	TRIOS 6®	.273*	.039	<0.001	.153	.392
		EPG	.338*	.090	.008	.057	.618
		iTero Lumina™	.322*	.039	<0.001	.203	.441
		i900®	.278*	.039	<0.001	.159	.398
		AoralScan Elite IPG®	.318*	.039	<0.001	.199	.438
	EPG	TRIOS 6®	−0.065	.090	1.000	−0.345	.215
		CS 3800®	−0.338*	.090	.008	−0.618	−0.057
		iTero Lumina™	−0.016	.090	1.000	−0.296	.265
		i900®	−0.059	.090	1.000	−0.339	.221
		AoralScan Elite IPG®	−0.019	.090	1.000	−0.299	.261
	iTero Lumina™	TRIOS 6®	−0.049	.039	1.000	−0.169	.070
		CS 3800®	−0.322*	.039	<0.001	−0.441	−0.203
		EPG	.016	.090	1.000	−0.265	.296
		i900®	−0.044	.039	1.000	−0.163	.076
		AoralScan Elite IPG®	−0.004	.039	1.000	−0.123	.116
	i900®	TRIOS 6®	−0.006	.039	1.000	−0.125	.114
		CS 3800®	−0.278*	.039	<0.001	−0.398	−0.159
		EPG	.059	.090	1.000	−0.221	.339

(*continued on next page*)

Table 6 (*continued*)

Measure: Points							
Factor1	(I) Technology	(J) Technology	Mean Difference (I-J)	Std. Error	Sig. [b]	95 % Confidence Interval for Difference [b]	
						Lower Bound	Upper Bound
		iTero Lumina™	.044	.039	1.000	−0.076	.163
		AoralScan Elite IPG®	.040	.039	1.000	−0.080	.159
	AoralScan Elite IPG®	TRIOS 6®	−0.045	.039	1.000	−0.165	.074
		CS 3800®	−0.318*	.039	<0.001	−0.438	−0.199
		EPG	.019	.090	1.000	−0.261	.299
		iTero Lumina™	.004	.039	1.000	−0.116	.123
		i900®	−0.040	.039	1.000	−0.159	.080
#16-#22	TRIOS 6®	CS 3800®	−0.364*	.031	<0.001	−0.458	−0.269
		EPG	.081	.072	1.000	−0.141	.303
		iTero Lumina™	.049	.031	1.000	−0.046	.143
		i900®	.001	.031	1.000	−0.093	.096
		AoralScan Elite IPG®	.031	.031	1.000	−0.064	.125
	CS 3800®	TRIOS 6®	.364*	.031	<0.001	.269	.458
		EPG	.445*	.072	<0.001	.222	.667
		iTero Lumina™	.412*	.031	<0.001	.317	.507
		i900®	.365*	.031	<0.001	.270	.460
		AoralScan Elite IPG®	.394*	.031	<0.001	.299	.489
	EPG	TRIOS 6®	−0.081	.072	1.000	−0.303	.141
		CS 3800®	−0.445*	.072	<0.001	−0.667	−0.222
		iTero Lumina™	−0.032	.072	1.000	−0.255	.190
		i900®	−0.080	.072	1.000	−0.302	.143
		AoralScan Elite IPG®	−0.050	.072	1.000	−0.273	.172
	iTero Lumina™	TRIOS 6®	−0.049	.031	1.000	−0.143	.046
		CS 3800®	−0.412*	.031	<0.001	−0.507	−0.317
		EPG	.032	.072	1.000	−0.190	.255
		i900®	−0.047	.031	1.000	−0.142	.047
		AoralScan Elite IPG®	−0.018	.031	1.000	−0.113	.077
	i900®	TRIOS 6®	−0.001	.031	1.000	−0.096	.093
		CS 3800®	−0.365*	.031	<0.001	−0.460	−0.270
		EPG	.080	.072	1.000	−0.143	.302
		iTero Lumina™	.047	.031	1.000	−0.047	.142
		AoralScan Elite IPG®	.029	.031	1.000	−0.065	.124
	AoralScan Elite IPG®	TRIOS 6®	−0.031	.031	1.000	−0.125	.064
		CS 3800®	−0.394*	.031	<0.001	−0.489	−0.299
		EPG	.050	.072	1.000	−0.172	.273
		iTero Lumina™	.018	.031	1.000	−0.077	.113
		i900®	−0.029	.031	1.000	−0.124	.065
#16-#26	TRIOS 6®	CS 3800®	.067	.048	1.000	−0.081	.215
		EPG	.337	.112	.062	−0.009	.683
		iTero Lumina™	.262*	.048	<0.001	.115	.410
		i900®	.209*	.048	.001	.061	.356
		AoralScan Elite IPG®	.280*	.048	<0.001	.132	.428
	CS 3800®	TRIOS 6®	−0.067	.048	1.000	−0.215	.081
		EPG	.270	.112	.294	−0.076	.616
		iTero Lumina™	.196*	.048	.003	.048	.343
		i900®	.142	.048	.070	−0.006	.289
		AoralScan Elite IPG®	.213*	.048	<0.001	.065	.361
	EPG	TRIOS 6®	−0.337	.112	.062	−0.683	.009
		CS 3800®	−0.270	.112	.294	−0.616	.076
		iTero Lumina™	−0.075	.112	1.000	−0.421	.271
		i900®	−0.129	.112	1.000	−0.475	.218
		AoralScan Elite IPG®	−0.057	.112	1.000	−0.403	.289
	iTero Lumina™	TRIOS 6®	−0.262*	.048	<0.001	−0.410	−0.115
		CS 3800®	−0.196*	.048	.003	−0.343	−0.048
		EPG	.075	.112	1.000	−0.271	.421
		i900®	−0.054	.048	1.000	−0.201	.094
		AoralScan Elite IPG®	.018	.048	1.000	−0.130	.165
	i900®	TRIOS 6®	−0.209*	.048	.001	−0.356	−0.061
		CS 3800®	−0.142	.048	.070	−0.289	.006
		EPG	.129	.112	1.000	−0.218	.475
		iTero Lumina™	.054	.048	1.000	−0.094	.201
		AoralScan Elite IPG®	.071	.048	1.000	−0.076	.219
	AoralScan Elite IPG®	TRIOS 6®	−0.280*	.048	<0.001	−0.428	−0.132
		CS 3800®	−0.213*	.048	<0.001	−0.361	−0.065
		EPG	.057	.112	1.000	−0.289	.403
		iTero Lumina™	−0.018	.048	1.000	−0.165	.130
		i900®	−0.071	.048	1.000	−0.219	.076
#22-#24	TRIOS 6®	CS 3800®	−0.048*	.012	.005	−0.086	−0.010
		EPG	.048	.029	1.000	−0.041	.138
		iTero Lumina™	.036	.012	.074	−0.002	.074
		i900®	.032	.012	.202	−0.006	.070
		AoralScan Elite IPG®	.026	.012	.586	−0.012	.064

(*continued on next page*)

Table 6 (*continued*)

Measure: Points							
Factor1	(I) Technology	(J) Technology	Mean Difference (I-J)	Std. Error	Sig. [b]	95 % Confidence Interval for Difference [b]	
						Lower Bound	Upper Bound
	CS 3800®	TRIOS 6®	.048*	.012	.005	.010	.086
		EPG	.096*	.029	.025	.007	.186
		iTero Lumina™	.084*	.012	<0.001	.046	.122
		i900®	.080*	.012	<0.001	.041	.118
		AoralScan Elite IPG®	.074*	.012	<0.001	.036	.112
	EPG	TRIOS 6®	−0.048	.029	1.000	−0.138	.041
		CS 3800®	−0.096*	.029	.025	−0.186	−0.007
		iTero Lumina™	−0.012	.029	1.000	−0.101	.077
		i900®	−0.017	.029	1.000	−0.106	.073
		AoralScan Elite IPG®	−0.022	.029	1.000	−0.112	.067
	iTero Lumina™	TRIOS 6®	−0.036	.012	.074	−0.074	.002
		CS 3800®	−0.084*	.012	<0.001	−0.122	−0.046
		EPG	.012	.029	1.000	−0.077	.101
		i900®	−0.005	.012	1.000	−0.043	.033
		AoralScan Elite IPG®	−0.010	.012	1.000	−0.048	.028
	i900®	TRIOS 6®	−0.032	.012	.202	−0.070	.006
		CS 3800®	−0.080*	.012	<0.001	−0.118	−0.041
		EPG	.017	.029	1.000	−0.073	.106
		iTero Lumina™	.005	.012	1.000	−0.033	.043
		AoralScan Elite IPG®	−0.006	.012	1.000	−0.044	.033
	AoralScan Elite IPG®	TRIOS 6®	−0.026	.012	.586	−0.064	.012
		CS 3800®	−0.074*	.012	<0.001	−0.112	−0.036
		EPG	.022	.029	1.000	−0.067	.112
		iTero Lumina™	.010	.012	1.000	−0.028	.048
		i900®	.006	.012	1.000	−0.033	.044
#22-#26	TRIOS 6®	CS 3800®	−0.174*	.022	<0.001	−0.243	−0.105
		EPG	.052	.052	1.000	−0.109	.214
		iTero Lumina™	.021	.022	1.000	−0.048	.090
		i900®	.000	.022	1.000	−0.069	.069
		AoralScan Elite IPG®	.050	.022	.428	−0.019	.119
	CS 3800®	TRIOS 6®	.174*	.022	<0.001	.105	.243
		EPG	.227*	.052	.001	.065	.388
		iTero Lumina™	.195*	.022	<0.001	.126	.264
		i900®	.174*	.022	<0.001	.105	.243
		AoralScan Elite IPG®	.224*	.022	<0.001	.156	.293
	EPG	TRIOS 6®	−0.052	.052	1.000	−0.214	.109
		CS 3800®	−0.227*	.052	.001	−0.388	−0.065
		iTero Lumina™	−0.032	.052	1.000	−0.193	.130
		i900®	−0.053	.052	1.000	−0.214	.109
		AoralScan Elite IPG®	−0.002	.052	1.000	−0.164	.159
	iTero Lumina™	TRIOS 6®	−0.021	.022	1.000	−0.090	.048
		CS 3800®	−0.195*	.022	<0.001	−0.264	−0.126
		EPG	.032	.052	1.000	−0.130	.193
		i900®	−0.021	.022	1.000	−0.090	.048
		AoralScan Elite IPG®	.029	.022	1.000	−0.040	.098
	i900®	TRIOS 6®	.000	.022	1.000	−0.069	.069
		CS 3800®	−0.174*	.022	<0.001	−0.243	−0.105
		EPG	.053	.052	1.000	−0.109	.214
		iTero Lumina™	.021	.022	1.000	−0.048	.090
		AoralScan Elite IPG®	.050	.022	.421	−0.018	.119
	AoralScan Elite IPG®	TRIOS 6®	−0.050	.022	.428	−0.119	.019
		CS 3800®	−0.224*	.022	<0.001	−0.293	−0.156
		EPG	.002	.052	1.000	−0.159	.164
		iTero Lumina™	−0.029	.022	1.000	−0.098	.040
		i900®	−0.050	.022	.421	−0.119	.018
#24-#26	TRIOS 6®	CS 3800®	−0.146*	.014	<0.001	−0.189	−0.102
		EPG	.009	.033	1.000	−0.093	.111
		iTero Lumina™	.000	.014	1.000	−0.044	.043
		i900®	−0.017	.014	1.000	−0.060	.027
		AoralScan Elite IPG®	.011	.014	1.000	−0.032	.055
	CS 3800®	TRIOS 6®	.146*	.014	<0.001	.102	.189
		EPG	.155*	.033	<0.001	.053	.257
		iTero Lumina™	.146*	.014	<0.001	.102	.189
		i900®	.129*	.014	<0.001	.085	.173
		AoralScan Elite IPG®	.157*	.014	<0.001	.114	.201
	EPG	TRIOS 6®	−0.009	.033	1.000	−0.111	.093
		CS 3800®	−0.155*	.033	<0.001	−0.257	−0.053
		iTero Lumina™	−0.009	.033	1.000	−0.111	.093
		i900®	−0.026	.033	1.000	−0.128	.076
		AoralScan Elite IPG®	.002	.033	1.000	−0.100	.104
	iTero Lumina™	TRIOS 6®	.000	.014	1.000	−0.043	.044
		CS 3800®	−0.146*	.014	<0.001	−0.189	−0.102

(*continued on next page*)

Table 6 (*continued*)

Measure: Points							
Factor1	(I) Technology	(J) Technology	Mean Difference (I-J)	Std. Error	Sig. [b]	95 % Confidence Interval for Difference [b]	
						Lower Bound	Upper Bound
		EPG	.009	.033	1.000	−0.093	.111
		i900®	−0.017	.014	1.000	−0.060	.027
		AoralScan Elite IPG®	.012	.014	1.000	−0.032	.055
	i900®	TRIOS 6®	.017	.014	1.000	−0.027	.060
		CS 3800®	−0.129*	.014	<0.001	−0.173	−0.085
		EPG	.026	.033	1.000	−0.076	.128
		iTero Lumina™	.017	.014	1.000	−0.027	.060
		AoralScan Elite IPG®	.028	.014	.753	−0.015	.072
	AoralScan Elite IPG®	TRIOS 6®	−0.011	.014	1.000	−0.055	.032
		CS 3800®	−0.157*	.014	<0.001	−0.201	−0.114
		EPG	−0.002	.033	1.000	−0.104	.100
		iTero Lumina™	−0.012	.014	1.000	−0.055	.032
		i900®	−0.028	.014	.753	−0.072	.015

Based on estimated marginal means.
* The mean difference is significant at the 0.05 level.
[b] Adjustment for multiple comparisons: Bonferroni.

with extraoral and intraoral approaches—seems to represent the most accurate method for digital FA implant capture, as reported in a recently published systematic review with meta-analysis [42]. However, direct acquisition with the iTero Lumina™ demonstrated high trueness, showing no statistically significant differences compared with IPG. These promising results may be clinically relevant, suggesting that this new generation of IOS is approaching the accuracy achieved by photogrammetric technologies. Finally, in the present study we included an older, discontinued IOS (CS 3800®) to evaluate differences in accuracy between previous and current-generation models, to assess the technological advances made over the past five years, and ultimately to highlight the importance of calibration procedures and software updates in a demanding application such as FA implant scanning.

This study has several limitations. It is an *in vitro* investigation conducted under experimental conditions, where the influence of saliva, blood, and potential patient head movements was eliminated [43]. Moreover, all scans were performed by a single highly experienced operator with over 15 years of intraoral scanning practice, which may have reduced the performance gap between direct IOS acquisitions and photogrammetric techniques. In addition, only a limited number of IOSs were evaluated, and further analyses including a wider range of devices available on the market are warranted, including, where possible, the most recent photogrammetry applications available for mobile phones [44]. Finally, EPG was performed with the plaster model outside the mannequin head, while IPG and direct IOS scanning were done with the model inside the mannequin; despite the external light conditions were carefully controlled, this may have had an effect, and therefore represent a limitation of the present study. For all these reasons, additional *in vitro* and clinical studies with broader and more diversified designs are necessary before drawing definitive conclusions regarding the use and validation of direct intraoral scanning for FA implant impressions.

Disclosure

Given his role as Section Editor of the Digital Dentistry Section of the Journal of Dentistry (or, Editor-in-chief of the Digital Dentistry Journal), Dr. Francesco Mangano had no involvement in the peer review of this article and had no access to information regarding its peer review. Full responsibility for the editorial process for this article was delegated to another journal editor.

Conflict of interest statement

The authors report no conflict of interest related to the present clinical study. The materials presented in the study belong to the authors, who have not received any grant or financial support for the preparation of the present research.

Video 1. Model acquisition using EPG (3Dots®, OpenTech, Brescia, Italy).

Video 2. The EPG software (3Dots®, OpenTech, Brescia, Italy) computes the spacial position of the implants.

CRediT authorship contribution statement

Francesco Guido Mangano: Writing – review & editing, Writing – original draft, Visualization, Project administration, Methodology, Investigation, Conceptualization. **Henriette Lerner:** Project administration, Funding acquisition. **Gabriele Valle:** Visualization, Validation, Software, Investigation, Data curation. **Francesco Biaggini:** Supervision, Resources, Project administration, Funding acquisition. **Carlo Mangano:** Writing – review & editing. **Andrey Dybov:** Writing – review & editing.

Declaration of competing interest

The authors report no conflict of interest related to the present clinical study. The materials presented in the study belong to the authors, who have not received any grant or financial support for the preparation of the present research.

Supplementary materials

Supplementary material associated with this article can be found, in the online version, at doi:10.1016/j.jdent.2025.106269.

References

[1] F. Mangano, Digital dentistry, J. Dent. 109 (2021) 103693, https://doi.org/10.1016/j.jdent.2021.103693.
[2] F. Eggmann, M.B. Blatz, The core of digital dentistry: intraoral scanners, Compend. Contin. Educ. Dent. 45 (2024) 503–507. PMID: 39561342.
[3] T. Joda, M. Ferrari, G.O. Gallucci, J.G. Wittneben, U. Bragger, Digital technology in fixed implant prosthodontics, Periodontol. 2000 73 (2017) 178–192, https://doi.org/10.1111/prd.12164.
[4] F. Mangano, G. Veronesi, Digital versus Analog procedures for the prosthetic restoration of single implants: a randomized controlled trial with 1 year of follow-up, Biomed. Res. Int. (2018) 5325032, https://doi.org/10.1155/2018/5325032, 2018.
[5] T. Joda, U. Bragger, N.U. Zitzmann, CAD/CAM implant crowns in a digital workflow: five-year follow-up of a prospective clinical trial, Clin. ImPlant Dent. Relat. Res. 21 (2019) 169–174, https://doi.org/10.1111/cid.12681.
[6] F.G. Mangano, C. Mangano, M. Loktionova, O. Dudnik, O. Malanova, A. Elovskaya, A. Maltseva, A. Dybov, Additively manufactured hybrid composite implant-supported restorations: a retrospective clinical study of 145 patients with up to 2

years of follow-up, J. Dent. 161 (2025) 105999, https://doi.org/10.1016/j.jdent.2025.105999.
[7] M. Pirc, S. Wenk, D. Peter, A. Ioannidis, R. Jung, T. Joda, Four-dimensional (4D) virtual simulation for predicting soft tissue support and vertical dimension of occlusion in full-arch implant therapy - A proof of concept, J. Dent. (2025) 106142, https://doi.org/10.1016/j.jdent.2025.106142. Oct 6Online ahead of print.
[8] N. Joensahakij, P. Serichetaphongse, W. Chengprapakorn, The accuracy of conventional versus digital (intraoral scanner or photogrammetry) impression techniques in full-arch implant-supported prostheses: a systematic review, Evid. Based. Dent. 25 (2024) 216–217, https://doi.org/10.1038/s41432-024-01045-z.
[9] A. Alfaraj, F. Alqudaihi, Z. Khurshid, O. Qadiri, W.S. Lin, Comparative analyses of accuracy between digital and conventional impressions for complete-arch implant-supported fixed dental prostheses- A systematic review and meta-analysis, J. Prosthodont. (2025), https://doi.org/10.1111/jopr.14094. Jul 14Online ahead of print.
[10] Y.J. Zhang, J.Y. Shi, S.J. Qian, S.C. Qiao, H.C. Lai, Accuracy of full-arch digital implant impressions taken using intraoral scanners and related variables: a systematic review, Int. J. Oral Implant. 14 (2021) 157–179. PMID: 34006079.
[11] V. Vitai, A. Nemeth, E. Solyom, L.M. Czumbel, B. Szabo, R. Fazekas, G. Gerber, P. Hegyi, P. Hermann, J. Borbely, Evaluation of the accuracy of intraoral scanners for complete-arch scanning: a systematic review and network meta-analysis, J. Dent. 137 (2023) 104636, https://doi.org/10.1016/j.jdent.2023.104636.
[12] M. Revilla-León, M. Gómez-Polo, V. Rutkunas, P. Ntovas, J.C. Kois, Classification of complete-arch implant scanning techniques recorded by using intraoral scanners, J. Esthet. Restor. Dent. 37 (2025) 236–243, https://doi.org/10.1111/jerd.13322.
[13] D.M. Elawady, M. Denewar, A.Y. Alqutaibi, W.I. Ibrahim, Clinical assessment of maxillary screw-retained implant prostheses fabricated from digital versus conventional full-arch implant impressions. A randomized controlled clinical trial, Int. J. Comput. Dent. 28 (2025) 151–161, https://doi.org/10.3290/j.ijcd.b5117247.
[14] M. Imburgia, J. Kois, E. Marino, H. Lerner, F.G. Mangano, Continuous scan strategy (CSS): a novel technique to improve the accuracy of intraoral digital impressions, Eur. J. Prosthodont. Restor. Dent. 28 (2020) 128–141, https://doi.org/10.1922/EJPRD_2105Imburgia14.
[15] F. Mangano, A. Gandolfi, G. Luongo, S. Logozzo, Intraoral scanners in dentistry: a review of the current literature, BMC. Oral Health 17 (2017) 149, https://doi.org/10.1186/s12903-017-0442-x.
[16] F.G. Mangano, O. Admakin, M. Bonacina, H. Lerner, V. Rutkunas, C. Mangano, Trueness of 12 intraoral scanners in the full-arch implant impression: a comparative in vitro study, BMC. Oral Health 20 (2020) 263, https://doi.org/10.1186/s12903-020-01254-9.
[17] M. Revilla-León, A. Lanis, B. Yilmaz, J.C. Kois, G.O. Gallucci, Intraoral digital implant scans: parameters to improve accuracy, J. Prosthodont. 32 (2023) 150–164, https://doi.org/10.1111/jopr.13749.
[18] G. Ochoa-López, R. Cascos, J.L. Antonaya-Martín, M. Revilla-León, M. Gómez-Polo, Influence of ambient light conditions on the accuracy and scanning time of seven intraoral scanners in complete-arch implant scans, J. Dent. 121 (2022) 104138, https://doi.org/10.1016/j.jdent.2022.104138.
[19] F. Grande, P. Nuytens, S. Zahabiyoun, O. Iocca, S. Catapano, E. Mijiritsky, Factors influencing the intraoral implant scan accuracy: a review of the literature, J. Dent. 161 (2025) 105973, https://doi.org/10.1016/j.jdent.2025.105973.
[20] P. Gehrke, M. Rashidpour, R. Sader, P. Weigl, A systematic review of factors impacting intraoral scanning accuracy in implant dentistry with emphasis on scan bodies, Int. J. ImPlant Dent. 10 (2024) 20, https://doi.org/10.1186/s40729-024-00543-0.
[21] M. Gómez-Polo, M.B. Donmez, G. Çakmak, B. Yilmaz, M. Revilla-León, Influence of implant scan body design (height, diameter, geometry, material, and retention system) on intraoral scanning accuracy: a systematic review, J. Prosthodont. 32 (2023) 165–180, https://doi.org/10.1111/jopr.13774.
[22] F. Grande, A. Mosca Balma, F. Mussano, S. Catapano, Effect of Implant Scan body type, intraoral scanner and Scan Strategy on the accuracy and scanning time of a maxillary complete arch implant scans: an in vitro study, J. Dent. 159 (2025) 105782, https://doi.org/10.1016/j.jdent.2025.105782.
[23] U. Hauschild, H. Lerner, P. Weigl, T. Porrà, O. Admakin, F.G. Mangano, Effects of the intraoral scanner and implant library on the trueness of digital impressions in the full-arch implant scan: a comparative in vitro study, J. Dent. 150 (2024) 105336, https://doi.org/10.1016/j.jdent.2024.105336.
[24] G. Michelinakis, D. Apostolakis, D. Nikolidakis, G. Lapsanis, Influence of different scan body design features and intraoral scanners on the congruence between scan body meshes and library files: an in vitro study, J. Prosthet. Dent. 132 (2024), https://doi.org/10.1016/j.prosdent.2024.05.016, 454.e1-454.e11.
[25] Y. Ashraf, A. Abo El Fadl, A. Hamdy, K. Ebeid, Effect of different intraoral scanners and scanbody splinting on accuracy of scanning implant-supported full arch fixed prosthesis, J. Esthet. Restor. Dent. 35 (2023) 1257–1263, https://doi.org/10.1111/jerd.13070.
[26] A. Pozzi, L. Arcuri, F. Lio, A. Papa, A. Nardi, J. Londono, Accuracy of complete-arch digital implant impression with or without scanbody splinting: an in vitro study, J. Dent. 119 (2022) 104072, https://doi.org/10.1016/j.jdent.2022.104072.
[27] F. Rustichini, R. Romolini, M.C. Salmi, L. Gennai, F. Vermigli, F.G. Mangano, Implant-supported full-arch fixed dental prostheses manufactured through a direct digital workflow using a calibrated splinting framework: a retrospective clinical study, J. Dent. 154 (2025) 105605, https://doi.org/10.1016/j.jdent.2025.105605.
[28] M. Klein, F.J. Tuminelli, A. Sallustio, G.D. Giglio, H. Lerner, R.W. Berg, A. Waltuch, Full-arch restoration with the NEXUS IOS system: a retrospective clinical evaluation of 37 restorations after a one year of follow-up, J. Dent. 139 (2023) 104741, https://doi.org/10.1016/j.jdent.2023.104741.
[29] K. Abuduwaili, R. Huang, J. Song, Y. Liu, Z. Chen, B. Huang, Z. Li, Comparison of photogrammetric imaging, intraoral scanning and conventional impression accuracy of full-arch dental implant rehabilitation: an in vitro study, BMC. Oral Health 25 (2025) 753, https://doi.org/10.1186/s12903-025-06029-8.
[30] W.M. Negreiros, T.C. Sun, S. Jain, M. Finkelman, G.O. Gallucci, A. Hamilton, Precision of complete-arch digital implant scans using photogrammetry and intra-oral scanning. An in vivo cross-over study: photogrammetry vs IOS, J. Dent. 161 (2025) 105928, https://doi.org/10.1016/j.jdent.2025.105928.
[31] C.P. Noronha, C. Ferreira de Souza, M. Dantas Dos Santos Oliveira, E.V.F.D. Silva, N. Sesma, M.K. Mukai, Accuracy of stereophotogrammetry in implant scanning compared to intraoral scanning in completely edentulous patients - A systematic review and meta-analysis, Int. J. Prosthodont. 0 (0) (2025) 1–20, https://doi.org/10.11607/ijp.9358. Jul 22Online ahead of print.
[32] A. Pozzi, L. Arcuri, P. Carosi, A. Laureti, J. Londono, H.L. Wang, Photogrammetry versus intraoral scanning in complete-arch digital implant impression: a systematic review and meta-analysis, Clin. ImPlant Dent. Relat. Res. 27 (2025), https://doi.org/10.1111/cid.70059 e70059.
[33] M. Estibalez-Recasens, C. Serrano-Granger, A. Santamaria-Laorden, C. Andreu-Vazquez, J. Orejas-Perez, Precision of stereophotogrammetry in complete arch implant recordings: a clinical study, J. Prosthet. Dent. 133 (2025) 1242–1249, https://doi.org/10.1016/j.prosdent.2024.12.021.
[34] M. Revilla-León, R. Cascos, A.B. Barmak, M. Drone, J.C. Kois, M. Gómez-Polo, Accuracy of complete arch implant scans recorded by using intraoral and extraoral photogrammetry systems and a non-calibrated splinting technique: a clinical study, J. Prosthet. Dent. (2025), https://doi.org/10.1016/j.prosdent.2025.07.027. Sep 10: S0022-3913(25)00647-XOnline ahead of print.
[35] J. Brakoč, A. Todorović, F.G. Mangano, M. Glišić, M. Šćepanović, Accuracy of intraoral photogrammetry versus direct digital implant impressions in the fully edentulous lower jaw: an in vitro study, J. Dent. 156 (2025) 105654, https://doi.org/10.1016/j.jdent.2025.
[36] M. Revilla-León, R. Cascos, A.B. Barmak, M. Drone, J.C. Kois, M. Gómez-Polo, Clinical accuracy of complete arch implant scans recorded by using a non-calibrated splinting technique, intraoral photogrammetry, and extraoral photogrammetry with snap-on markers, J. Prosthet. Dent. (2025), https://doi.org/10.1016/j.prosdent.2025.09.012. Sep 25: S0022-3913(25)00736-XOnline ahead of print.
[37] J. Buhl, A. Ender, A. Mehl, Accuracy of current intraoral scanning systems for full-arch impressions: an in vitro study, J. Dent. 161 (2025) 105984, https://doi.org/10.1016/j.jdent.2025.105984.
[38] A.B. Nulty, An In vivo comparison of trueness and precision of two novel methods for improving edentulous full arch implant scanning accuracy: a pilot study, Dent. J. (Basel) 12 (2024) 367, https://doi.org/10.3390/dj12110367.
[39] I. Baresel, J. Baresel, Full arch accuracy of intraoral scanners with different acquisition technologies: an in vitro study, J. Dent. 156 (2025) 105703, https://doi.org/10.1016/j.jdent.2025.105703.
[40] M. Revilla-León, M. Gómez-Polo, M. Drone, A.B. Barmak, J.C. Kois, J. Alonso Pérez-Barquero, Accuracy of complete arch implant scans recorded by using intraoral and extraoral photogrammetry systems, J. Prosthet. Dent. (2025), https://doi.org/10.1016/j.prosdent.2025.01.041. Online ahead of print.
[41] X.J. Fu, Z.Z. Cai, J.Y. Shi, S.C. Qiao, M.S. Tonetti, H.C. Lai, B.L. Liu, Accuracy of a novel intraoral photogrammetry technique for complete-arch implant impressions: an in vitro study, Clin. Oral Implants Res. 36 (2025) 991–999, https://doi.org/10.1111/clr.14445.
[42] H. Atalla, H. Alhelou, F. Karaduman, O. Alawawda, F. Bayindir, Comparative accuracy of photogrammetry and intraoral scanners in recordings for complete arch implant-supported prostheses: a systematic review and meta-analysis, J. Prosthet. Dent. (2025), https://doi.org/10.1016/j.prosdent.2025.10.059. Nov 14:S0022-3913(25)00864-9Online ahead of print.
[43] D. Borbola, G. Berkei, B. Simon, L. Romanszky, G. Sersli, M. DeFee, W. Renne, F. Mangano, J. Vag, In vitro comparison of five desktop scanners and an industrial scanner in the evaluation of an intraoral scanner accuracy, J. Dent. 129 (2023) 104391, https://doi.org/10.1016/j.jdent.2022.104391.
[44] A. Santamaría-Laorden, A.M. Marugán, C. Andreu-Vázquez, J. Orejas-Pérez, Complete arch implant capture using a photogrammetry algorithm and smartphone app: an in vitro study, J. Dent. 161 (2025) 105969, https://doi.org/10.1016/j.jdent.2025.105969.